Eur. J. Mineral.
2015, **27**, 311–323
Published online 27 February 2015

**"Characterization, diagnosis and conservation of cultural heritage". School held in Catania/Siracusa, 1st to 4th July 2014**

# Lime mortar consolidation with nanostructured calcium hydroxide dispersions: the efficacy of different consolidating products for heritage conservation

ANNA ARIZZI[1,2,*], LUZ STELLA GOMEZ-VILLALBA[3], PAULA LOPEZ-ARCE[3,4], GIUSEPPE CULTRONE[1] and RAFAEL FORT[3]

[1] Departamento de Mineralogía y Petrología, Universidad de Granada, Avda. Fuentenueva s/n, 18002 Granada, Spain
[2] School of Geography and the Environment, University of Oxford, Dyson Perrins Building, South Parks Road, Oxford OX1 3QY, UK
*Corresponding author, e-mail: anna.arizzi@ouce.ox.ac.uk
[3] Instituto de Geociencias (IGEO, CSIC-UCM), José Antonio Nováis 12, 28040 Madrid, Spain
[4] Géosciences et Environnement, Université de Cergy-Pontoise, 5, Gay-Lussac - Rue d'Eragny, Neuville-sur-Oise, 95031 Cergy-Pontoise cedex, France

**Abstract:** This paper analyses the efficacy of dispersions of nanoparticles of calcium hydroxide for consolidating lime mortars, according to three variables: the type of dispersion (three consolidating compounds—CaLoSil®, Nanorestore® and Merck®—with different-sized calcium hydroxide particles); the concentration of the dispersion (5 and 25 g/L of $Ca(OH)_2$ in isopropyl alcohol); and the state of the sample (comparison of saturated and non-saturated samples). The outcome of the consolidation process was studied in terms of improved carbonation of the mortar, mineralogy (by means of X-ray diffraction and thermogravimetric analyses), texture (study of the porosity by mercury intrusion porosimetry) and compactness (measurement of ultrasonic velocity propagation through samples). To ensure that the treatment had no negative effects on the physical characteristics of the mortars, we performed microstructural (phase morphology studied by means of scanning electron microscopy) and aesthetic (colour and lightness measured by spectrophotometry) analyses. Of the different dispersions, CaLoSil® at 5 g/L produced the most significant improvement in the degree of carbonation and in the compactness of the mortar, thanks to the precipitation of small crystals of calcite and aragonite in the pores located between the matrix and the aggregate grains. This product also caused the least significant chromatic changes (slight decrease in lightness and yellowing) and the greatest increase in ultrasonic propagation velocity through the mortar samples. This research has specific application in restoration work that involves consolidation of lime mortars, especially in tropical climates or in confined environments with high humidity levels (such as deep hypogea).

**Key-words:** lime mortars; calcium hydroxide; nanoparticles; consolidation; heritage conservation.

## 1. Introduction

In the last decade, application of nanotechnology to the conservation of artistic and architectural heritage has aroused great interest amongst scientists, conservators and archaeologists (Baglioni & Giorgi, 2006), and various synthetic routes have been designed to obtain nanoparticles of calcium hydroxide for conservation purposes (*e.g.* Giorgi *et al.*, 2000; Salvadori & Dei, 2001; Daniele *et al.*, 2008; Rodriguez-Navarro *et al.*, 2013). The dispersion of $Ca(OH)_2$ nanoparticles in alcohol has been shown to be an effective consolidating product for many types of works of art, especially frescoes (Ambrosi *et al.*, 2001; Baglioni *et al.*, 2014), and building stone (Dei & Salvadori, 2006; Daniele & Taglieri, 2010; López-Arce *et al.*, 2010; Chelazzi *et al.*, 2013; Rodriguez-Navarro *et al.*, 2013; Licchelli *et al.*, 2014; Ruffolo *et al.*, 2014). Due to their colloidal character (*i.e.* nanometric size) and depending on the alcohol used as a solvent, $Ca(OH)_2$ particles can penetrate a few millimetres inside the material (Giorgi *et al.*, 2000) where they react with atmospheric $CO_2$ (*i.e.* carbonation process) to produce calcium carbonate ($CaCO_3$). The precipitated product acts as a binder giving the decayed material a more cohesive texture. When this method is used to consolidate damaged frescoes for example, it increases the cohesion between the layers of paint and the adhesion of the pigment grains to the substrate (Ambrosi *et al.*, 2001; Dei & Salvadori, 2006). In building stones, this treatment reinforces the texture and re-aggregates the powdering surfaces (Dei & Salvadori, 2006). Furthermore, when compared to other consolidating compounds, such as polymeric resins, nano-dispersions of $Ca(OH)_2$ show higher physical-chemical and physical-mechanical compatibility with the original materials as well as better durability and reversibility (Matteini &

DOI: 10.1127/ejm/2015/0027-2437
0935-1221/15/0027-2437 $ 5.85

Moles, 2003; Carretti *et al.*, 2013). The consolidating ability of $Ca(OH)_2$ nano-dispersions depends on their stability and on extrinsic factors, such as relative humidity and exposure time, which directly influence the carbonation velocity and the precipitation of calcium carbonate polymorphs, such as vaterite and aragonite, which are less stable than calcite (Gomez-Villalba *et al.*, 2011; Lopez-Arce *et al.*, 2011).

The consolidating ability of dispersions of calcium hydroxide nanoparticles has also been used recently in the treatment of deteriorated bones, thanks to the presence of collagen, which promotes the precipitation of aragonite (Natali *et al.*, 2014).

Drdácky *et al.* (2014) stated that the consolidation of mortars has rarely been quantitatively assessed. Although there are a range of studies on the consolidation of mural paintings, most of them carried out by Dei and co-workers (CSGI group, *Center for Colloid and Surface Science*, http://silicon.csgi.unifi.it/), relatively few studies have been made of non-painted or non-decorated renders and plasters (*i.e.* mortar that covers external or internal wall surfaces) (Borsoi *et al.*, 2012; Azeteiro *et al.*, 2014). This is not surprising, considering the higher cultural and artistic value of murals and given that renders and plasters in poor condition are usually removed, either in part or entirely, and replaced with new mortar. However, there are certain specific cases in which an ancient plaster or render cannot be removed or in which the damage is not so severe as to require removal; in these cases, consolidation is the most appropriate treatment.

The main decay phenomena affecting renders and plasters include: loss of cohesion between the matrix and aggregate grains, resulting in powdering and loss of material; loss of adhesion to the substrate and between the rendering layers; lime leaching; formation of shrinkage fissures, with worsening of the mechanical and hydric properties of the mortar; and attack by soluble salts and pollutants (Henry & Stewart, 2011). Apart from this last decay factor, which requires further specific action, and depending on the degree of damage suffered by the material, consolidation is often an effective solution for increasing the compactness of the decaying mortar.

One possible treatment for consolidating renders is grouting (Azeteiro *et al.*, 2014), although it is normally used for filling empty internal cavities in the wall to solve structural problems. In the case of plasters and renders that are a few centimetres thick, the best consolidating process in terms of compatibility involves the application of calcium hydroxide nanoparticles dispersed in alcohol, because the mortar matrix (lime-based) has the same chemical composition as the consolidating product. Furthermore, since renders and plasters tend to suffer the same decay problems as mural paintings, the methodology used for consolidating such paintings can be extrapolated to plasters and renders. There are, however, some differences that cannot be disregarded, for example: in a layer of render, the grading of the aggregate grains is usually larger and the binder-to-aggregate proportion is richer in aggregate than in lime, compared to the layer of mortar applied as a base for a mural. As a result, the renders have totally different textures, especially in terms of open porosity and pore size distribution, both factors that affect the carbonation process and the degree to which the consolidating compound penetrates the render.

In view of the above, we decided to investigate the consolidation of lime mortars using commercial dispersions of calcium hydroxide particles. In this paper we study the different outcomes of the consolidation process according to the following three variables:

(1) the type of dispersion: mortar samples treated with three different dispersions of calcium hydroxide particles at the same concentration.
(2) the concentration of the dispersion: mortar samples treated with the same type of dispersion at two different concentrations.
(3) the state of the sample: comparison of previously saturated and non-saturated samples treated with the same dispersion.

In the first two stages we analysed and compared the behaviour of three commercial consolidating products (CaLoSil®, Nanorestore® and Merck®), which differ above all in terms of particle size. In Stage 2 we used one of the dispersions (CaLoSil®) to investigate to what extent the concentration of the dispersion affects the penetration depth of the product in samples and any differences there may be in terms of physical changes.

In Stage 3 we investigated how the state of the sample influences the outcome of the consolidation process. In mortars that are not yet fully hardened, such as in samples that have been curing for 28 days, water moving through the matrix may lead to a partial dissolution of portlandite (from the lime) in the pore water and its re-precipitation (Arizzi & Cultrone, 2014), thus modifying the mortar microstructure (pore size distribution and cohesion between lime and aggregate). This aspect needs to be taken into account when studying the efficacy of a consolidation process on ''young'' mortar samples. For this reason, half of the samples treated with one type of dispersion (CaLoSil at 5 g/L) were saturated under water and then dried before consolidation. We then compared them with the remaining samples, which had not been saturated prior to the treatment. These tests on samples that are not fully hardened are important because uncarbonated mortars can still be found in ancient buildings decades or even centuries after application (Ferretti & Bazant, 2006). When a protective feature of the building (*e.g.* roof covering, pointing mortar) fails, the uncarbonated mortar can leach out due to rain penetration, leading to changes in the masonry surface or, in the worst cases, to the formation of voids (Henry & Stewart, 2011). In these cases, these non-fully carbonated mortars must be consolidated to prevent aesthetic damage or instability in the building.

The outcome of the consolidation process has been studied in terms of the improvement of the degree of carbonation, the texture and compactness of the mortar, while at the same time ensuring that the microstructural (phase morphology) and aesthetic (colour and lightness) characteristics are not harmed by the treatment.

It is worth highlighting that during consolidation, samples were exposed to high relative humidity (RH ∼ 90 %), so as to ensure faster carbonation (Gomez-Villalba *et al.*, 2011; Lopez-Arce *et al.*, 2011). This makes this study a useful reference for consolidating processes carried out on lime mortars used in buildings located in tropical regions and in confined environments with an unusual microclimate, such as hypogea, where relative humidity can sometimes exceed 90 % (in deep hypogea with high water content and no air movement, Cardinale *et al.*, 2010).

## 2. Materials and methods

### 2.1. Lime mortar samples

Mortars were prepared with a dry hydrated lime (CL90S, UNE-EN 459–1, 2002, supplied by ANCASA, Seville, Spain) and a fine crushed calcareous aggregate ($0.063 < ø < 1.5$ mm, produced in the Darro plant, Granada, Spain), in a lime-to-aggregate proportion of 1:3 by weight. In total, 13 cylindrical samples (4 cm height and 3 cm diameter) were prepared following the European standard (UNE-EN, 1015–2, 1999) and cured at 20 ± 5°C and RH = 60 ± 5 % for 28 days before consolidation. One of these cylindrical samples was cut to obtain two cubic pieces (1 $cm^3$) from the surface (*surf*) and the core (*core*) of the mortar, as shown in Fig. 1.

### 2.2. Types of dispersion

Four calcium hydroxide dispersions were selected to consolidate mortar samples:

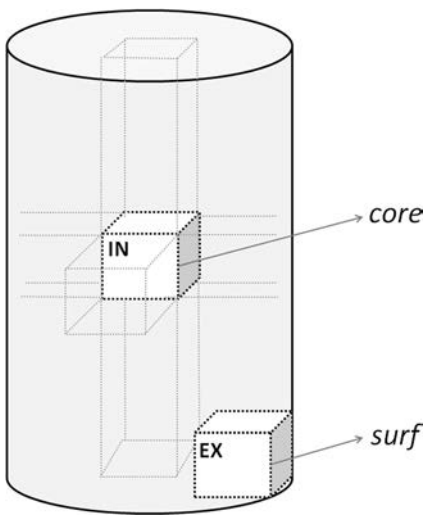


Fig. 1. Scheme of the external (EX) and internal (IN) zone where *surface* and *core* samples (1 $cm^3$) were collected, respectively, from one cylindrical sample after 28 days curing.

- CaLoSil® (Ziegenbald, 2008). From the commercial colloidal precursor, two dispersions of calcium hydroxide were prepared at different concentrations (5 and 25 g/L) in isopropyl alcohol. These dispersions were called CS5 and CS25, respectively. This product was previously characterized by Gomez-Villalba *et al.* (2012a) and consists of disaggregated hexagonal nanoparticles with particle size ranging from 60 to 130 nm.
- Nanorestore®, developed at the University of Florence (CSGI Consortium, Dei & Salvadori, 2006). This dispersion, consisting of plate-like nanocrystals of calcium hydroxide (<100 nm in size, Lopez-Arce *et al.*, 2011), was prepared at a concentration of 5 g/L in isopropyl alcohol. This dispersion was called NR5.
- Merck® calcium hydroxide particles (around 900 nm in size) dispersed in isopropyl alcohol at a concentration of 5 g/L, referred to here as MK5.

The four dispersions were left for 5 min in an ultrasonic bath to disperse the particles (Selecta model Ultrasounds-H) before being used.

### 2.3. Consolidation treatment of mortar samples

The dispersions were absorbed into the mortar samples by capillary absorption. The amount of dispersion used was established by taking the amount of water that the mortar absorbs during total immersion as the maximum saturation value. The consolidation methodology and amount of product were chosen according to the most appropriate application method determined by Zornoza-Indart *et al.* (2012) for carbonate stones. Since saturated samples absorbed up to 10 mL of water, the same quantity of dispersion was used for consolidating each of the 12 cylindrical mortar samples, although given the different methods of absorption (total immersion under water at atmospheric pressure for saturation and capillary uptake for consolidation), we did not expect the samples to absorb as much product. For the consolidation of the *surf*CS5 and *core*CS5 samples, only 2 mL of dispersion was used because they are approximately 1/5 the size of the cylindrical samples.

All samples were placed in individual glass beakers, with one face in contact with the dispersion, and were left for 8 weeks in a partially closed desiccator, used as a climatic chamber. The relative humidity inside the chamber was controlled by a RH sensor (Onset Hobo data logger). The RH of 90 ± 5 % was reached by placing a container with water in the bottom of the chamber, so as to simulate a humid environment. To prevent the water from coming into contact with the samples, the beakers and watch glasses were placed on a grille several centimetres above the bottom. The air conditioning system inside the room stabilized the temperature ($T$) at 19 ± 1°C. The $CO_2$ concentration inside the chamber (5 ppm) was registered by a $CO_2$ detector (Ventostat 8002, Telaire, Goleta, CA,

USA). The $CO_2$ concentration in the room where the samples were placed is usually 500 ± 100 ppm. However, the low value of 5 ppm recorded during consolidation of the samples in the partially ventilated chamber could be due to consumption of $CO_2$ by the samples during the consolidation process.

The same procedure was undertaken with the two cubic samples (EX and IN) although they were consolidated only with the CS5 dispersion. A blank untreated sample was left under the same conditions of *T*, RH and $CO_2$ concentration to evaluate the modifications resulting from the carbonation of the lime already present in the mortar as a binder. Ten millilitres of each type of dispersion were also put onto separate watch glasses and kept under the same conditions until the end of the study. Table 1 illustrates the consolidation conditions for each sample. Some samples were saturated under water and oven-dried before the treatment so as to investigate the water absorption capacity of the mortars before and after consolidation.

After 8 weeks of treatment, the mortar samples were weighed and oven-dried for 24 h at 30°C and 20 % RH; they were then put in a desiccator and finally stored in sealed plastic bags to prepare them for the physical characterization. The dispersions were studied using scanning electron microscopy (as detailed below), without being previously oven-dried.

### 2.4. Study before and after the consolidation treatment

Mortar samples were characterized before and after consolidation to assess the modifications in terms of mineralogy and petrophysical properties. To investigate the efficacy of the consolidation treatment across the sample, both the exterior (EX) and the interior (IN) areas of the cylindrical samples were characterized using the following techniques.

The mineralogy of the samples and dispersions was studied by means of X-ray diffraction (XRD) analysis, using a Panalytical X'Pert PRO MPD diffractometer, with automatic loader. Analysis conditions were: radiation Cu$K\alpha$ ($\lambda = 1.5405$ Å), 3 to 60°2θ explored area, 45 kV voltage, 40 mA current intensity and goniometer speed using a Si-detector X'Celerator of 0.01°2θ/s. Identification of the mineral phases was performed using first the X-Powder© software (Martin Ramos, 2004) and then the PCPDFWIN database. The amount of calcium hydroxide and carbonates in the samples was calculated by thermogravimetric analysis (TGA), using a SHIMADZU TGA-50H analyser, which worked in a $N_2$ atmosphere, at a heating rate of 10°C/min over a range of 25–950°C. Approximately 70 mg of sample were ground before the analysis. This technique allowed us to determine the degree of carbonation ($I_{CD}$, in %), according to the following equation (Arizzi & Cultrone, 2014):

$$I_{CD} = \frac{CH_0 - CH_x}{CH_0} \times 100 \quad (1)$$

where $CH_x$ is the amount of calcium hydroxide at time *x* and $CH_0$ is the initial content of calcium hydroxide (at time 0).

High-resolution field-emission scanning electron microscopy (FESEM) was performed to study the mineral phase morphology, using a Carl Zeiss SMT AURIGA microscope, operating at 4 kV for the mortar samples and 2 kV for dispersions. Samples were carbon-coated before observation.

Mercury intrusion porosimetry (MIP) was carried out to determine mortar porosity ($P_o$, %) and pore size distribution (PSD, in a pore diameter range of $0.005 < d < 400$ μm),

Table 1. Conditions of consolidation: sample number, name and shape; type, concentration and amount of dispersion used; water saturation before and after consolidation. *surf*, external cubic sample obtained from a cylindrical one; *core*, internal cubic sample obtained from a cylindrical one.

| Sample name | Sample shape | Type of dispersion and concentration(g/L) | Amount of dispersion | Water saturation *before* | Water saturation *after* |
|---|---|---|---|---|---|
| *CS5_1* | cylindrical | CaLoSil®, 5 | 10 mL | yes | no |
| *CS5_2* | cylindrical | CaLoSil®, 5 | 10 mL | yes | yes |
| *CS25_3* | cylindrical | CaLoSil®, 25 | 10 mL | yes | no |
| *CS25_4* | cylindrical | CaLoSil®, 25 | 10 mL | yes | yes |
| *NR5_5* | cylindrical | Nanorestore®, 5 | 10 mL | yes | no |
| *NR5_6* | cylindrical | Nanorestore®, 5 | 10 mL | yes | yes |
| *MK5_7* | cylindrical | Merck®, 5 | 10 mL | yes | no |
| *MK5_8* | cylindrical | Merck®, 5 | 10 mL | yes | yes |
| *BLANK_9* | cylindrical | – | – | yes | no |
| *BLANK_10* | cylindrical | – | – | yes | yes |
| *CS5_11* | cylindrical | CaLoSil®, 5 | 10 mL | no | no |
| *CS5_12* | cylindrical | CaLoSil®, 5 | 10 mL | no | yes |
| *surfCS5* | cubic | CaLoSil®, 5 | 2 mL | no | no |
| *coreCS5* | cubic | CaLoSil®, 5 | 2 mL | no | no |
| *CS5-blank* | dispersion | CaLoSil®, 5 | 10 mL | – | – |
| *CS25-blank* | dispersion | CaLoSil®, 25 | 10 mL | – | – |
| *NR-blank* | dispersion | Nanorestore®, 5 | 10 mL | – | – |
| *MK-blank* | dispersion | Merck®, 5 | 10 mL | – | – |

at conditions ranging from atmospheric pressure to 60,000 psia (414 MPa) using a Micromeritics Autopore IV 9500 porosimeter. Mortar fragments of *ca*. 1 $cm^3$ were oven-dried for 24 h at 30°C and 20 % RH before MIP analysis.

Ten cylindrical samples were saturated under water and oven-dried before consolidation. Half of these samples were also saturated and oven-dried again after consolidation, so as to evaluate any possible changes in the water absorption capacity of the mortar. The variation in the mass after saturation under water was calculated as follows:

$$\Delta M = \frac{M_s - M_d}{M_d} \times 100 \quad (2)$$

where $M_s$ is the mass of the sample after saturation and $M_d$ is the dry mass of the sample.

One sample (CS5_12) was only saturated after consolidation (Table 1), so as to investigate possible differences in the consolidation process between the non-saturated and the saturated samples treated with the same dispersion (CaLoSil®, 5g/L). Water saturation was performed by total immersion of oven-dried ($T = 30$°C and RH = 20 % for 24 hours) samples in deionised water, until the mass variation was less than 0.1 %.

The ultrasonic velocity propagation ($V_p$) through mortars was measured both on saturated and non-saturated samples. P-wave propagation time was measured to a precision of 0.1 μs with a PUNDIT CNS Electronics instrument, following the European standard recommendations UNE-EN 14579 (2005). The frequency of the transducers used was 1 MHz with a diameter of 9 mm. Measurements were taken in direct transmission/reception mode, across opposite parallel sides of the specimens.

Finally, a Konica-Minolta CM-700d spectrophotometer was used to determine the overall colour difference (ΔE*) of the samples before and after consolidation, according to the following equation:

$$\Delta E^* = \sqrt{\left((L_1^* - L_2^*)^2 + (a_1^* - a_2^*)^2 + (b_1^* - b_2^*)^2\right)} \quad (3)$$

where $L_1$*, $a_1$* and $b_1$* are the lightness and the chromatic coordinates of the untreated samples and $L_2$*, $a_2$* and $b_2$* are those of samples after consolidation, respectively. $L$*, $a$* and $b$* were measured according to the CIELab system, at the following working conditions: 3 mm diameter of the measured area, D65 illuminant, 10° view angle, SCI/SCE mode and 400–700 nm light radiation range. The colour was measured at four points in each sample.

Environmental scanning electron microscopy (ESEM) was performed on the cubic samples (*surf*CS5 and *core*CS5) using a Quanta 200 FEI microscope equipped with an energy dispersive X-ray detector (EDX) from Oxford Instrument Analytical, and the UK-INCA system, operating in low-vacuum mode at 20 kV. Two faces of these samples were observed by means of ESEM before and after consolidation: the bottom face, in contact with the dispersion, and the side face, parallel to the capillary front (Fig. 2). In the latter, three areas were distinguished and their position saved in order to be able to clearly determine the penetration depth of the dispersion after consolidation (Fig. 2).

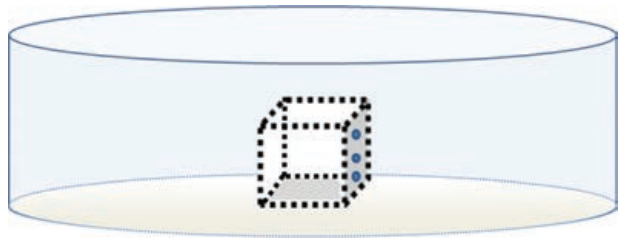

Fig. 2. Scheme of the cubic sample (1 $cm^3$) in contact with the CS5 dispersion during consolidation. The bottom and the side face are represented in grey; the three points on the side face represent the three zones observed by ESEM before and after consolidation.

After ESEM observations, the mineralogy of *surf*CS5 and *core*CS5 samples was analysed by means of XRD and TGA, at the same conditions described above.

## 3. Results and discussion

### 3.1. General remarks on the consolidation treatment

In many samples all of the dispersion was absorbed during the first day of treatment, although in samples NR5_5 and NR5_6 (treated with NR5), MK5_7 (treated with MK5), CS5_11 and CS_12 (treated with CS5 but not saturated under water and oven-dried before consolidation) and *surf*CS5 and *core*CS5, a small amount of dispersion was still present in the bottom of the beaker. During the first 24 h, indeed, a $CO_2$ concentration of 0 ppm was registered, indicating that the $CO_2$ had been consumed during the transformation of the calcium hydroxide into calcium carbonate. After 48 h, small amounts of dispersion were still present in the beakers with samples CS5_11, CS5_12, *surf*CS5 and *core*CS5. After 72 h, all the beakers were dry, although the watch glasses took a further week to dry (the 2 week of treatment). At the end of the consolidation process (after 8 weeks), the bottom face of samples CS25_3 and CS25_4 (treated with CS25) showed a solid white dry layer, indicating that the dispersion had deposited mainly on the bottom of the samples. For this reason, in CS25 samples both the top (a) and the bottom (b) parts of the samples were studied by XRD and TGA, to investigate possible differences in carbonation due to a lower penetration depth in this sample compared to the others.

### 3.2. Results for the different dispersions

Figure 3 shows the XRD patterns obtained for each dispersion after 8 weeks exposure at 90 % RH. In all dispersions carbonation has been achieved, obtaining similar behaviour when the consolidating compounds are at a concentration of 5 g/L. In these XRD patterns (Fig. 3a), indeed, all peaks are

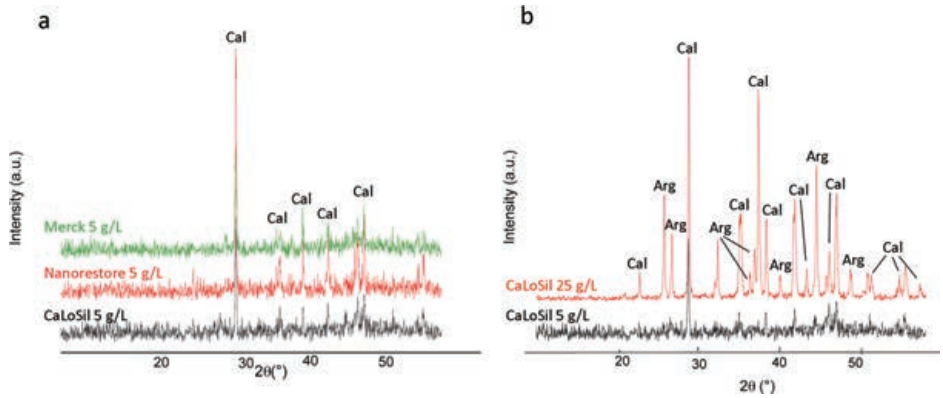


Fig. 3. X-ray diffraction patterns of the consolidating dispersions after 8 weeks exposure at 90 % RH. CaLoSil, Nanorestore and Merck dispersions at 5 g/L (a); CaLoSil dispersions at 5 g/L and 25 g/L (b). Arg, aragonite; Cal, calcite.

assigned to calcite, although the broad shape of the profiles suggests that they may also contain aragonite in smaller concentrations (Gomez-Villalba *et al.*, 2011; López-Arce *et al.*, 2011). The XRD patterns of CaLoSil at 5 g/L and 25 g/L (Fig. 3b) show differences in the polymorphs: peaks can be assigned to calcite and aragonite in the 25 g/L sample and to calcite in the 5 g/L case. This may be related to different concentration and exposure conditions within the chamber, which caused a gradient in the aragonite–calcite transformation. This process may be affected by small fluctuations in the supply of $CO_2$ and humidity around the particles (Gomez-Villalba *et al.*, 2012a).

Figure 4 shows the FESEM images for consolidating products after 8 weeks at 90 % RH. In CaLoSil dispersion at 5 g/L (Fig. 4a), calcite in the form of non-aggregated tabular crystals with uniform size (137–571 nm) was identified. In CaLoSil dispersion at 25 g/L (Fig. 4b) two types of crystals were identified: acicular crystals of aragonite (1.788–2.797 μm) and tabular crystals of calcite (217–538 nm). In Nanorestore dispersion at 5 g/L (Fig. 4c) different forms of calcite were identified: scalenohedra (1.015 to 2.36 μm), tabular aggregates (54–89 nm) and rhombohedral crystals (432–1196 nm). Finally, in the Merck dispersion at 5 g/L (Fig. 4d), calcite in the form of scalenohedral, columnar (518–1308 nm) and tabular (262–402 nm) crystals was identified. The identification of these phases on the basis of their morphology corroborates the XRD results (Fig. 3).

The XRD and FESEM observations highlighted various differences between the three consolidating products. Although they all have the same composition, the state of carbonation, the particle size and the particle morphology vary.

The first difference was noted with the different concentration levels (the CaLoSil 5 g/L and 25 g/L dispersions). After 8 weeks of exposure at 90 % RH, the

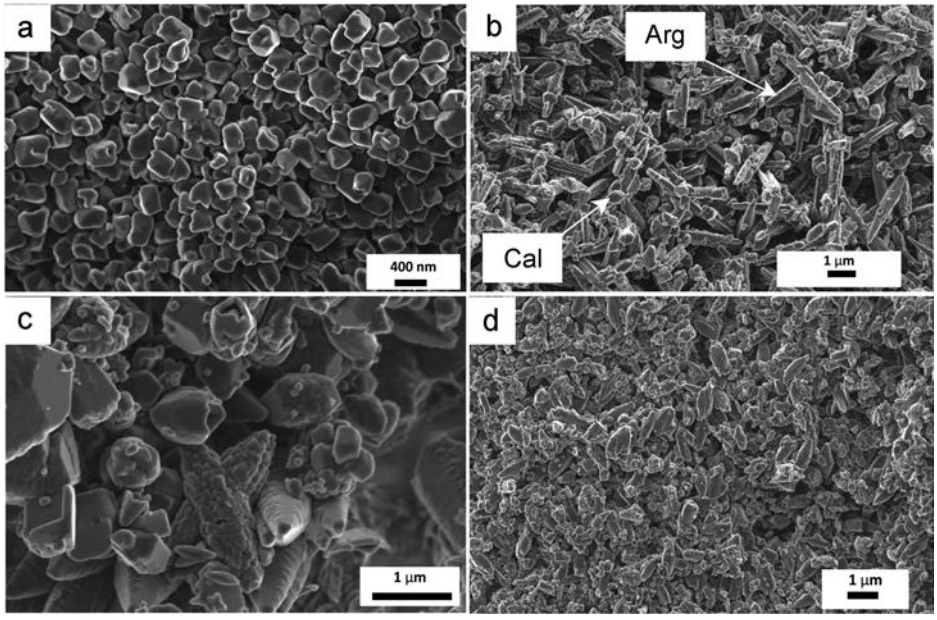


Fig. 4. FESEM images of CaLoSil 5 g/L (a), CaLosil 25 g/L (b), Nanorestore 5 g/L (c) and Merck 5 g/L (d) dispersions after 8 weeks exposure at 90 % RH. Arg, aragonite; Cal, calcite.

dispersion with the smallest and most homogeneous particle size was CaLoSil 5 g/L. Another interesting result was that this product only shows the presence of calcite, the most stable phase within $CaCO_3$ polymorphs at room conditions. In the more concentrated solution (CaLoSil 25 g/L), differences in the $CO_2$ concentration or the water vapour pressure around the particles (Gomez-Villalba *et al.*, 2012a) generated two polymorphs: the larger, less stable aragonite, with micrometric particles, and calcite, in smaller nanometric particles.

The product with the lowest uniformity in terms of particle size (ranging between 1 and 2 μm) is Nanorestore 5 g/L. However, carbonation has also been reached, achieving the most stable phase, calcite, which developed in different sizes and shapes indicating different growth stages.

Merck 5 g/L dispersion also achieved carbonation although, considering the initial (average 900 nm) and final (1.5 μm) particle size, the growth of calcite crystals was slower compared to NR and CS dispersions (Gomez-Villalba *et al.*, 2012b).

### 3.3. Study of mortar samples after treatment

#### *3.3.1. Degree of carbonation and mineralogy*

As shown in Table 2, very similar results were obtained from the quantification of the calcium hydroxide (CH or Por, portlandite) and calcium carbonate (CC) phases using XRD and TGA. Thermogravimetric analysis cannot differentiate between the carbonate polymorphs, which means that only the total amount of calcium carbonates (TOT CC in Table 2) could be calculated with this technique. XRD by contrast can distinguish between and quantify the amounts of aragonite (Arg) and calcite (Cal). Vaterite was not identified by this technique. Only TGA was used to determine the degree of carbonation (Eq. 1).

The exposure of the untreated samples (BLANK) to the *T*, RH and $CO_{2\ conc}$ conditions of the chamber led to a great improvement in their degree of carbonation, which increased by 62 ± 4 % (BLANK_9, Table 2). The degree of carbonation of the treated samples also changed due to consolidation. As expected, the surface of the samples (_EX) is more carbonated than the interior (_IN), as was the case in the untreated samples. However, the degree of carbonation inside the samples remains almost unvaried after the consolidation process ($I_{CD}$ of _IN ∼ 80 %, Table 2), except in previously non-saturated CS5 samples, where the degree of carbonation increased ($I_{CD}$ of CS5_11_IN 93 %, Table 2). This suggests that saturating the samples under water before the treatment may have decreased the availability of portlandite to $CO_2$ inside the samples during the consolidation process. Partial dissolution and re-precipitation processes that take place inside the pores during water absorption and drying (Arizzi & Cultrone, 2014) may be responsible for this phenomenon.

Of the three different products, CaLoSil induced the highest degree of carbonation, in particular when applied at a concentration of 5 g/L. The *surf*CS5 and *core*CS5 samples, also treated with CaLoSil 5 g/L, reached the highest degree of carbonation ($I_{CD}$ = 100 %) thanks to

Table 2. Mineral phases, carbonation degree index ($I_{CD}$) and open porosity ($P_o$, in %) of samples, studied by means of X-ray diffraction (XRD), thermogravimetric analysis (TGA) and mercury intrusion porosimetry (MIP). n.d., not determined; mortar *BC*, mortar sample before consolidation; EX, external zone; IN, internal zone; CH, calcium hydroxide; Por, portlandite; CC, calcium carbonates $CaCO_3$; Arg, aragonite; Cal, calcite; a, sample bottom; b, sample top; –, 0 %; tr, <2 %; *: 3–8 %; **: 9–14 %; ***: 15–25 %; +: 75–85 %; ++: 86–98 %. Standard deviation of $P_o$ values is approximately ±1.0.

| | | XRD/TGA | | | | | |
|---|---|---|---|---|---|---|---|
| | | | CC | | | TGA | MIP |
| Sample name | Age of samples (weeks) | Por/CH | Arg | Cal | TOT CC | $I_{CD}$ (%) | $P_o$ (%) |
| *mortar BC_EX* | 4 | *** | – | + | + | 25 | 37.6 |
| *mortar BC_IN* | 4 | n.d. | n.d. | n.d. | n.d. | n.d. | 39.3 |
| *CS5_1_EX* | 12 | * | – | ++ | ++ | 95 | 32.8 |
| *CS5_1_IN* | 12 | *** | – | + | + | 83 | 21.3 |
| *CS25_3_EX_a* | 12 | * | – | ++ | ++ | 96 | 36.3 |
| *CS25_3_EX_b* | 12 | *** | – | + | + | 85 | |
| *CS25_3_IN* | 12 | *** | – | + | + | 83 | 37.3 |
| *NR5_5_EX* | 12 | *** | – | + | + | 85 | 37.1 |
| *NR5_5_IN* | 12 | *** | – | + | + | 79 | 39.8 |
| *MK5_7_EX* | 12 | ** | – | ++ | ++ | 90 | 22.3 |
| *MK5_7_IN* | 12 | *** | – | + | + | 83 | 36.4 |
| *BLANK_9_EX* | 12 | ** | – | ++ | ++ | 91 | 37.1 |
| *BLANK_9_IN* | 12 | *** | – | + | + | 83 | 19.8 |
| *surf* | 12 | tr | * | ++ | ++ | 100 | n.d. |
| *core* | 12 | tr | * | ++ | ++ | 100 | n.d. |
| *CS5_11_ EX* | 12 | * | * | ++ | ++ | 97 | 31.5 |
| *CS5_11_ IN* | 12 | * | * | + | ++ | 93 | 36.3 |

the small size of these samples, which permitted easy diffusion of $CO_2$ through the sample.

The CaLoSil dispersion at 25 g/L only produced an increased degree of carbonation at the bottom of the sample where it was deposited during the treatment. Indeed in the $I_{CD}$ value for the exterior of this sample there is a difference of 10 %, between the reading taken at the bottom (CS25_3_EX_a, Table 2) and the top (CS25_3_EX_b, Table 2). This indicates that this dispersion was too concentrated to be absorbed by capillary uptake, and that it reached a lower penetration depth in samples 3 and 4 compared to the other samples treated with the same dispersion at lower concentration (samples CS5_1, CS5_2, CS5_11 and CS5_12).

According to the XRD results, both aragonite and calcite were present in the CS25 dispersion, whereas only calcite was identified in the CS5 solution (Fig. 3b). Considering the different solubilities of the two polymorphs it is also possible that differences during the capillary rise are related to the simultaneous presence of both polymorphs in CS25, in addition to the higher concentration.

Treating samples with micro-sized particles of calcium hydroxide (Merck dispersion at 5 g/L concentration) did not induce any improvement in the degree of carbonation, whilst the application of Nanorestore at 5 g/L concentration slowed down the hardening of samples, as indicated by the lower $I_{CD}$ values observed in samples NR5_5_EX and _IN (Table 2), compared to the untreated samples.

As a result of the carbonation process, treated mortars show calcite levels of between 75 wt% and 95 wt% (Cal, Table 2). In CS5_11, *surf*CS5 and *core*CS5 samples, which show the highest degree of carbonation, about 5 wt% of aragonite (Arg, Table 2) precipitated after the $Ca(OH)_2$ reacted with atmospheric $CO_2$. The presence of aragonite may be due to the fact that it precipitates under high RH conditions, above 75 % RH and especially around 90 % (Gomez-Villalba *et al.*, 2011; Lopez-Arce *et al.*, 2011).

### 3.3.2. *Open porosity and pore size distribution*

The porosity of untreated samples only decreased in the interior of the samples (by about 20 %, BLANK, Table 2), whilst it remained constant on the exterior, compared to the values determined before the study (BC, Table 2). The open porosity of the surface of samples (_EX) treated with a consolidating product is usually lower (but equal in the case of NR samples) than that of the untreated external sample (Table 2), indicating that the dispersion caused a partial closing of the pores in this area. The opposite was found in the interior of the treated samples, which always had a higher porosity than that detected inside the untreated samples (BLANK_9_IN, Table 2). The only exception was the CS5_1_IN sample, which has a similar open porosity value as the BLANK_9_IN sample.

According to the pore size distribution curves for the samples (Fig. 5), the majority of pores have diameters between 0.2 and 2 μm, typical of aerial lime-based mortars (Arandigoyen *et al.*, 2005; Lawrence *et al.*, 2007). Another family of pores has diameters between 0.01 and 0.1 μm; these pores usually form after the precipitation of calcium carbonate within the main pores (Lawrence *et al.*, 2007). Finally, a third family of pores of smaller volume and with diameters of more than 2 μm were recognised in the PSD curves. These pores are located in the contact zone between the matrix and the aggregate (ITZ, interfacial transition zone), and their volume usually decreases with carbonation (Arizzi & Cultrone, 2014). As shown in the PSD curves (Fig. 5), the pores at the ITZ are only present in samples before consolidation (BC) and in untreated samples (BLANK). This indicates that, in treated samples, the consolidating product induced the precipitation of calcium carbonate in this area, thus improving the adhesion between the matrix and the aggregate. Another clear modification of the pore system induced by the consolidation process is the decrease, on the mortar surface, of the volume of pores with diameters of 0.02–0.05 μm, especially in samples treated with Merck dispersion (MK, Fig. 5). The surface of this sample showed very low porosity ($P_o$ of MK5_7_EX $\sim$ 20 %, Table 2) compared to the other surface samples ($P_o \sim 35$ %, Table 2). This indicates that larger particles (*i.e.* those of almost micrometric size) penetrated less than the smaller ones of CaLoSil, so consolidating the surface more than the interior of the mortars.

The only case in which the volume of the smallest pores remained almost unchanged in both the exterior and the interior was in the samples treated with Nanorestore (NR, Fig. 5).

### 3.3.3. *Phase morphology and texture*

*3.3.3.1. Cylindrical samples studied by FESEM. BLANK*: The exterior of the untreated sample is much more compact and has smaller crystals than the interior (Fig. 6_blank_a). Only calcite has precipitated in the mortar matrix due to carbonation, in the form of nanometric (up to 300 nm in size) tabular and rhombohedral crystals (Fig. 6_blank_b). Many micrometric portlandite crystals are still present inside the blank mortar (Fig. 6_blank_c), in agreement with the XRD and TGA results (Table 2).

*CS5, non-saturated before treatment*: The exterior of samples treated with CaLoSil 5g/L and not previously saturated under water shows a compact matrix (Fig. 6_CS5_a) composed mainly of rhombohedral and scalenohedral calcite crystals (Fig. 6_CS5_b), which are larger than those found in the blank sample (Fig. 6_blank_b). The interior, by contrast, still has many micrometric portlandite crystals (from the binder) and a more porous matrix.

*CS5, saturated before treatment*: The mortar samples saturated before treatment experienced various textural and morphological changes, which differ from the non-saturated samples, even though they were treated with the same dispersion (CaLoSil 5 g/L). The first difference can be seen in the calcite crystals, which are smaller and more dispersed in the CS5 saturated samples (Fig. 6_CS5_c, up to 300 nm) compared to the non-saturated ones (Fig. 6_CS5_b, up to almost 1 μm). The second main difference relates to the growth, only in previously saturated samples, of needle-like aragonite crystals (Fig. 6_CS5_d, up to 3 μm

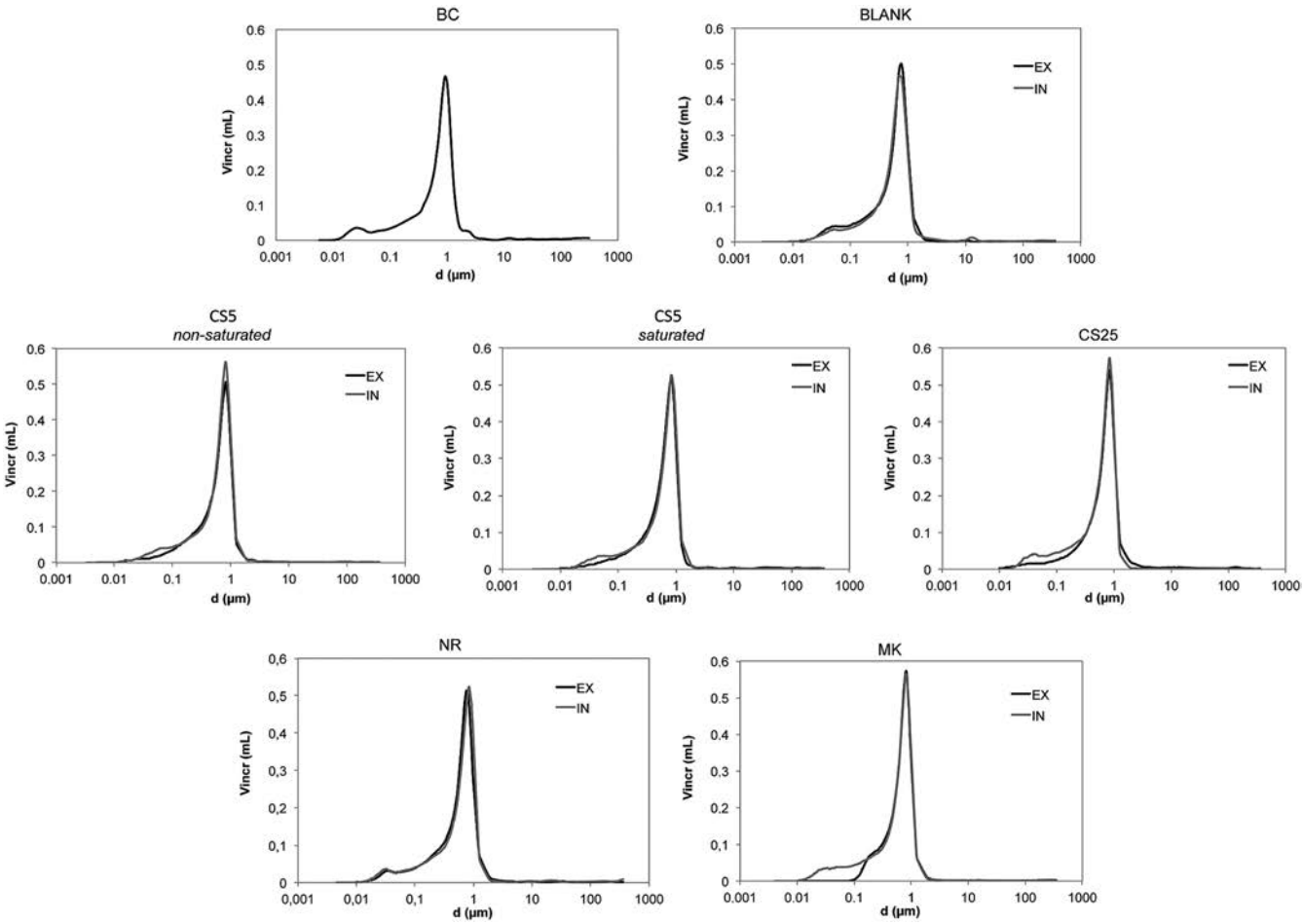


Fig. 5. Pore size distribution curves of the external samples of the cylindrical mortars: before consolidation (BC); untreated (BLANK); treated with CaLoSil 5 g/L (CS), Nanorestore 5 g/L (NR) and Merck 5 g/L (MK) dispersions after 8 weeks exposure at 90 % RH. The incremental pore volume ($V_{incr}$, in mL) is represented as a function of the pore diameter (d, in µm).

long), similar to those observed in dispersions of $Ca(OH)_2$ nanoparticles used to consolidate carbonate stone samples under high humidity conditions (75 % RH, Lopez-Arce *et al.*, 2010).

*CS25*: Due to the higher density of the CaLoSil dispersion at 25 g/L, a consolidated, fissured ''crust'' (Fig. 6_CS25_a) forms on the bottom of the cylindrical samples. When we looked at the matrix from the bottom part of the CS25 sample, we observed many needle-like aragonite crystals (about 1 µm in size) (Fig. 6_CS25_b), which were not identified by XRD (Table 2). This coincides with the dispersion of CaLoSil at 25 g/L in which the growth of acicular aragonite crystals was also observed (Fig. 4b). These crystals are similar in shape to those observed by the authors in previous research (Lopez-Arce *et al.*, 2011). Longer acicular crystals of aragonite (up to 2 µm) and clusters of calcite in the form of a rose were also observed on the bottom of the sample (Fig. 6_CS25_c). In the top part of the same sample only tabular calcite crystals were observed, similar in size to those observed in the blank sample (Fig. 6_blank_c). The fact that the presence of a crust and the growth of aragonite were only observed on the bottom of the sample suggest that the CaLoSil dispersion at 25 g/L was too concentrated to be absorbed by the sample by capillary uptake. Moreover, the similarity in the texture and morphology of the top part of this sample compared to the blank suggests that the consolidating product penetrated only 2–3 cm (cylindrical samples were 4 cm high). This is also supported by the fact that there was a lower degree of carbonation ($I_{CD}$, Table 2) in the CS25_3_EX_b (top) and CS25_3_IN samples compared to CS25_3_EX_a (bottom).

*NR*: The matrix of samples treated with Nanorestore shows very similar texture and morphology compared to the blank sample (Fig. 6_BLANK_a). In the same way, many micrometric portlandite crystals coming from the binder (Fig. 6_NR) are observed in the interior of the NR samples. Only calcite was identified in this sample, where it occurs in the form of tabular rather than scalenohedral crystals, in contrast with what was observed in the dispersion alone (Fig. 4c).

*MK*: Samples treated with the Merck product are also very similar to the blank, although the matrix of MK samples is slightly less compact; many calcite agglomerates and portlandite crystals are visible (Fig. 6_MK).

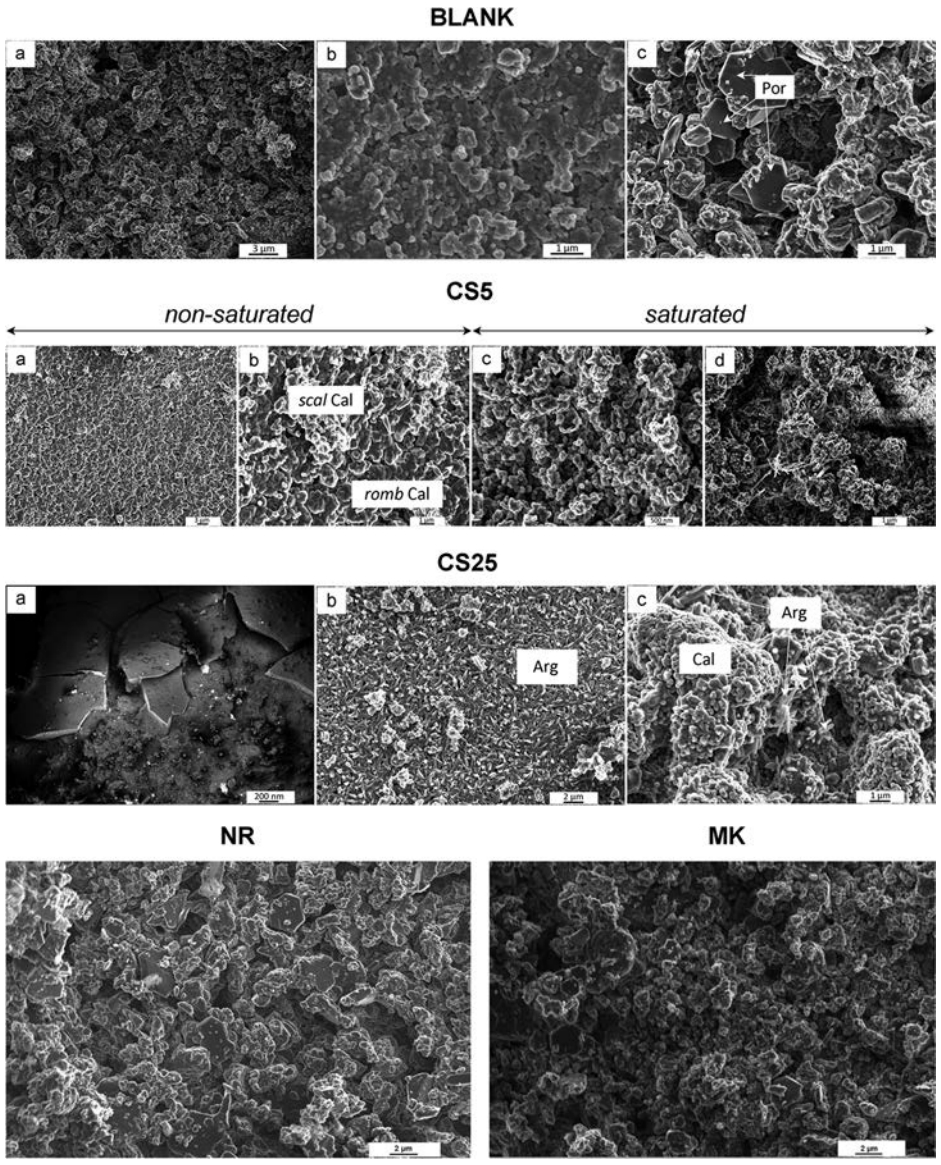


Fig. 6. FESEM images of cylindrical mortar samples: untreated (BLANK); treated with CaLoSil 5 g/L (CS5, saturated and non-saturated), CaLoSil 25 g/L (CS25), Nanorestore 5g/L (NR) and Merck 5 g/L (MK) dispersions after 8 weeks exposure at 90 % RH. Por: portlandite; Arg, aragonite; Cal: calcite; *scal* Cal, scalenohedral calcite; *romb* Cal: rhombohedral calcite.

The observations about the NR and MK samples coincide with the XRD and TGA results, which showed similar or slightly lower degrees of carbonation for MK5_7 and NR5_5 samples compared to the untreated ones (BLANK_9, Table 2).

*3.3.3.2. Cubic samples studied by ESEM.* If we compare the same areas of the cubic samples (treated with CaLoSil 5 g/L) before and after consolidation, it is evident that the treatment improved mortar texture and compactness (Fig. 7). Although the sample surface appears rougher after the treatment, most of the voids are filled with the carbonates that precipitated after consolidation (Fig. 7a) and the compactness and density of the matrix appear to be greatly improved (Fig. 7b). In particular, the treatment increased the cohesion at the interface between the matrix and the aggregate (images of two contact zones: Fig. 7c). Calcium carbonate precipitated in the form of needle-like crystals typical of aragonite (Fig. 7d) and as rhombohedral calcite crystals (Fig. 7e). In the cubic samples, aragonite appears in larger amounts than in the cylindrical samples (where present), as also confirmed by the XRD data (Table 2).

### *3.3.4. Physical-mechanical properties and water absorption ability*

Table 3 shows the values for colour variation (ΔE*), which includes changes in lightness (*L**) and chromatic parameters (*a** and *b**) after consolidation. In general, *L** values slightly decrease, whereas *a** and *b** values increase. Mortar samples treated with CaLoSil dispersion

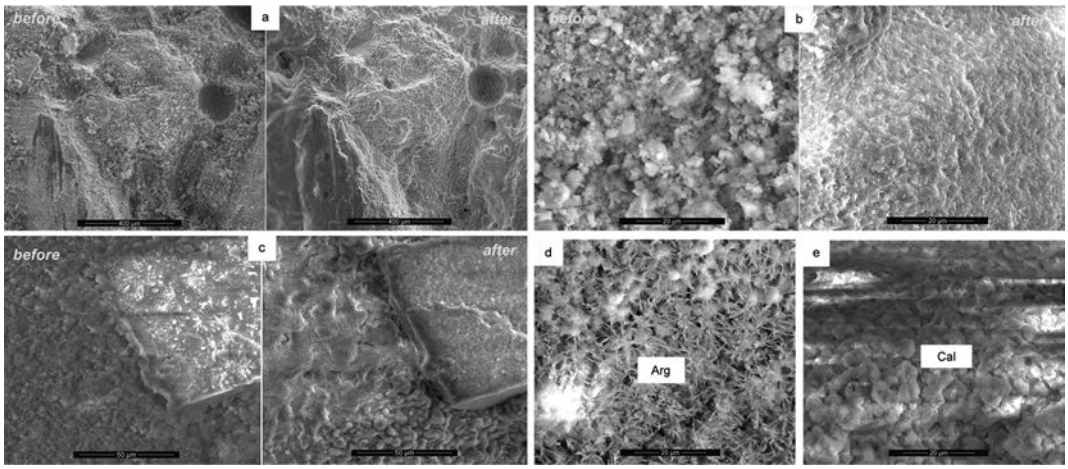


Fig. 7. ESEM images of areas of the same cubic sample before and after treatment with CaLoSil dispersion at 5 g/L. Arg, aragonite; Cal, calcite. Scales bars are 400 μm (a), 20 μm (b, d, e) and 50 μm (c).

at 5 g/L did not show significant chromatic variations. Their ΔE* values are less than 3 (CS5 samples, Table 3), indicating that the chromatic variation is not visible with the human eye (Boutin & Leroux, 2000). The other dispersions (Nanorestore and Merck), by contrast, produced more significant colour changes, with ΔE* values ranging between 4 and 6 (Table 3), which represents a medium-high risk of chromatic incompatibility between the original and the treated mortar (Rodrigues & Grossi, 2007).

The ultrasonic velocity propagation through the mortars increased in the untreated samples as a result of carbonation. The consolidation process, however, induced only a slightly higher increase in the $V_p$ values of samples, compared to the blank (Table 3 and in Fig. S1, freely available online as Supplementary Material linked to this article on the GSW website of the journal, http://eurjmin.geoscienceworld.org/).

The propagation of ultrasonic waves is slightly faster in previously non-saturated samples (11 and 12, Table 3), even though they have higher porosity values than the saturated samples (Table 2). It is worth highlighting that while only calcite precipitated in non-saturated samples (CS5_11 and _12), both calcite and aragonite were found in the saturated ones (CS5_1 and _2). Considering that ultrasonic waves are sensitive to phase changes, such as different media (solid-liquid-gaseous) or minerals (Arizzi *et al.*, 2013), it is possible that their velocity decreases when travelling through different carbonate polymorphs, due to differences in density, morphology (rhombohedral calcite and acicular aragonite) and size. This would explain why the ultrasonic velocity is higher in samples CS5_11 and 12.

The $\Delta M/M$ values (determined according to Eq. 3) in Table 3 show that all samples have a slightly lower absorption ability after the treatment (ΔM/M decreases by $\sim 1$ %), although this seems to be related only to the natural carbonation process that samples undergo in the chamber, as the ΔM/M values are similar to those for the blank sample (Table 3).

Table 3. Values of colour variation (ΔE*), propagation velocity of primary waves through non-saturated mortar samples ($V_p$, in m/s, with standard deviation of values) and mass variation after saturation under water ($\Delta M/M$, in %), measured on untreated (*before*) and treated (*after*) samples.

| | | $V_p$ | | ΔM/M | |
|---|---|---|---|---|---|
| Sample name | ΔE* | *before* | *after* | *before* | *after* |
| *CS5_1* | 2.19 | 1615 ± 39 | 1732 ± 33 | 24.19 | – |
| *CS5_2* | 3.63 | 1614 ± 38 | 1679 ± 36 | 23.13 | 22.18 |
| *CS25_3* | 4.47 | 1613 ± 20 | 1669 ± 16 | 23.01 | – |
| *CS25_4* | 2.54 | 1665 ± 33 | 1767 ± 83 | 22.85 | 21.73 |
| *NR5_5* | 4.06 | 1581 ± 45 | 1735 ± 53 | 23.02 | – |
| *NR5_6* | 5.58 | 1587 ± 6 | 1735 ± 33 | 23.51 | 22.23 |
| *MK5_7* | 5.80 | 1618 ± 18 | 1725 ± 50 | 23.70 | – |
| *MK5_8* | 3.96 | 1590 ± 34 | 1698 ± 72 | 23.09 | 22.12 |
| *BLANK_9* | 4.46 | 1569 ± 23 | 1656 ± 48 | 23.05 | – |
| *BLANK_10* | 3.45 | 1620 ± 50 | 1638 ± 179 | 23.01 | 21.98 |
| *CS5_11* | 1.06 | 2098 ± 78 | 1968 ± 85 | – | – |
| *CS5_12* | 3.35 | 1712 ± 103 | 1803 ± 33 | – | 22.23 |

## 4. Conclusions

This is the first study that tackles the consolidation process of lime-based mortars from three different but interrelated points of view.

We began by comparing the consolidating efficacy of three commercial dispersions of calcium hydroxide at 5 g/L in isopropyl alcohol. The CaLoSil® dispersion was found to be a more effective consolidating compound than the Nanorestore® and Merck® dispersions, in that it induced the highest degree of carbonation, decreased mortar porosity and made the matrix more compact thanks to the formation of densely aggregated rhombohedral calcite crystals and needle-like aragonite crystals (the latter precipitated because of the high relative humidity, 90 ± 5 %), especially at the interface between the matrix and the aggregate grains, whose adhesion was greatly improved. By contrast, neither the Nanorestore® nor the Merck® dispersions significantly improved the degree of carbonation or the textural characteristics of the mortar samples. The reason for the stronger consolidating effect shown by CaLoSil® must be related to the fact that its starting colloidal particles are smaller and more homogeneous in size and more dispersed than Nanorestore® and Merck®. By studying the carbonation of these dispersions at a relative humidity of 90 ± 5 % for 8 weeks, we found that the $CaCO_3$ particles that precipitated in CaLoSil® at 5 g/L are the smallest and most homogeneous in size when compared with those for Nanorestore® and Merck®.

The second question analysed was the effect of concentration on the penetration depth and consolidating power of calcium hydroxide particles, for which we used two different concentrations of CaLoSil® dispersion (5 and 25 g/L). Mortar samples treated with CaLoSil at 25 g/L were scarcely and unevenly consolidated, as demonstrated by differences in the degree of carbonation, phase morphology and matrix texture between the bottom (where the dispersion was deposited) and the top (not reached by the dispersion) of samples. At higher concentration, a much larger amount of aragonite precipitated in the dispersion.

We also analysed the influence of the state of mortar samples, finding that the efficacy of the consolidating treatment may vary as a result of the changes induced by the movement of water through the mortar matrix. Mortars are very heterogeneous materials whose characteristics change over time, due to the presence of small amounts of non-carbonated binder in the matrix, which can either carbonate or dissolve in water during wetting and re-precipitate within pores during drying. These phenomena need to be taken into account when performing *in situ* consolidation, where it is impossible to prevent groundwater capillary uptake and moisture condensation in the mortar being treated.

This study has demonstrated that consolidating products that are widely used on works of art with great success may not be as effective when applied to other materials or under different conditions. This shows that it is essential to test the different consolidating products before choosing the most appropriate for the particular material that requires treatment, as recommended in Article 10 of the Venice Charter (1964): ‘‘ *( . . . ) the consolidation of a monument can be achieved by the use of any modern technique for conservation and construction, the efficacy of which has been shown by scientific data and proved by experience*’’.

**Acknowledgements:** This research was funded by the GEOMATERIALES 2 (S2013/MIT-2914) research project supported by the Government of the Community of Madrid and the MAT-2012-34473 project, supported by the Spanish research group RNM179 of the Junta de Andalucía. The authors are grateful to Laura Tormo and Marta Furió of the Natural Science Museum (CSIC) for providing the ESEM photographs and analyses. Special thanks go to Andrés Lira Aguado for his support with the MIP analyses and to Ainara Zornoza Indart for her help with the environmental measurements.

## References

Ambrosi, M., Dei, L., Giorgi, R., Neto, C., Baglioni, P. (2001): Colloidal particles of $Ca(OH)_2$: properties and applications to restoration of frescoes. *Langmuir*, **17**, 4251–4255.

Arandigoyen, M., Pérez Bernal, J.L., Bello López, M.A., Alvarez, J.I. (2005): Lime-pastes with different kneading water: pore structure and capillary porosity. *Appl. Surf. Sci.*, **252**, 1449–1459.

Arizzi, A. & Cultrone, G. (2014): The water transfer properties and drying shrinkage of aerial lime-based mortars: an assessment of their quality as repair rendering materials. *Environ. Earth Sci.*, **71**, 1699–1710.

Arizzi, A., Martinez-Martinez, J., Cultrone, G. (2013): Ultrasonic wave propagation through lime mortars: an alternative and non-destructive tool for textural characterization. *Mater. Struct.*, **46**, 1321–1335.

Azeteiro, L.C., Velosa, A., Paiva, H., Mantas, P.Q., Ferreira, V.M., Veiga, R. (2014): Development of grouts for consolidation of old renders. *Constr. Build. Mater.*, **50**, 352–360.

Baglioni, P. & Giorgi, R. (2006): Soft and hard nanomaterials for restoration and conservation of cultural heritage. Review. *Soft Matter*, **2**, 293–303.

Baglioni, P., Chelazzi, D., Giorgi, R., Carretti, E., Toccafondi, N., Jaidar, Y. (2014): Commercial $Ca(OH)_2$ nanoparticles for the consolidation of immovable works of art. *Appl. Phys. A*, **114**, 723–732.

Borsoi, G., Tavares, M., Veiga, R., Santos Silva, A. (2012): Microstructural characterization of consolidant products for historical renders: an innovative nanostructured lime dispersion and a more traditional ethyl silicate limewater solution. *Microsc. Microanal.*, **18**, 1181–1189.

Boutin, F. & Leroux, L. (2000): Color and weight evolution of limestones protected by water repellents after a three-year ageing period in urban conditions. Proceedings of the 9th International Congress on deterioration and conservation of stone. E. Vasco Fassina, Elsevier, 197–205.

Cardinale, N., Rospi, G., Stazi, A. (2010): Energy and microclimatic performance of restored hypogeous buildings in south Italy: the ‘‘Sassi’’ district of Matera. *Build. Environ.*, **45**, 94–106.

Carretti, E., Chelazzi, D., Rocchigiani, G., Baglioni, P., Poggi, G., Dei, L. (2013): Interactions between nanostructured calcium

hydroxide and acrylate copolymers: implications in cultural heritage conservation. *Langmuir*, **29**, 9881–9890.

Chelazzi, D., Poggi, G., Jaidar, Y., Toccafondi, N., Giorgi, R., Baglioni, P. (2013): Hydroxide nanoparticles for cultural heritage: consolidation and protection of wall paintings and carbonate materials. *J. Colloid Interface Sci.*, **392**, 42–49.

Daniele, V. & Taglieri, G. (2010): Nanolime suspensions on natural lithotypes: the influence of concentration and residual water content on carbonatation process and on treatment effectiveness. *J. Cult. Herit.*, **11**, 102–106.

Daniele, V., Taglieri, G., Quaresima, R. (2008): The nanolimes in cultural heritage conservation: characterisation and analysis of the carbonation process. *J. Cult. Herit.*, **9**, 294–301.

Dei, L. & Salvadori, B. (2006): Nanotechnology in cultural heritage conservation: nanometric slaked lime saves architectonic and artistic surfaces from decay. *J. Cult. Herit.*, **7**, 110–115.

Drdácky, M., Lesák, J., Niedoba, K., Valach, J. (2014): Peeling tests for assessing the cohesion and consolidation characteristics of mortar and render surfaces. *Mater. Struct.*, doi:10.1617/s11527-014-0285-8

Ferretti, D. & Bazant, Z.P. (2006): Stability of ancient masonry towers: moisture diffusion, carbonation and size effect. *Cem. Concr. Res.*, **36**, 1379–1388.

Giorgi, R., Dei, L., Baglioni, P. (2000): A new method for consolidating wall paintings based on dispersions of lime in alcohol. *Stud. Conserv.*, **45**, 154–161.

Gomez-Villalba, L.S., Lopez-Arce, P., Alvarez de Buergo, M., Fort, R. (2011): Structural stability of a colloidal solution of $Ca(OH)_2$ nanocrystals exposed to high relative humidity conditions. *Appl. Phys. A*, **104**, 1249–1254.

—, —, —, — (2012a): Atomic defects and their relationship to aragonite-calcite transformation in portlandite nanocrystal carbonation. *Cryst. Growth Des.*, **12**, 4844–4852.

Gomez-Villalba, L.S., López-Arce, P., Zornoza-Indart, A., Alvarez de Buergo, M., Fort, R. (2012b): Modern restoration products based on nanoparticles: the case of the nanolime, interaction and compatibility with limestone and dolostones surfaces, advantages and limitations. *Geophys. Res. Abstr.*, **14**, EGU2012-2418. 2012 EGU General Assembly

Henry, A. & Stewart, J. (2011): Mortars, renders and plasters. *in* ''English heritage, practical building conservation'', Martin B. & Wood C., eds. Ashgate Publishing Limited, Farnham (UK), 121–153.

Lawrence, R.M., Mays, T.J., Rigby, S., Walker, P., D'Ayala, D. (2007): Effects of carbonation on the pore structure of non-hydraulic lime mortars. *Cem. Concr. Res.*, **37**, 1059–1069.

Licchelli, M., Malagodi, M., Weththimumi, M., Zanchi, C. (2014): Nanoparticles for conservation of bio-calcarenite stone. *Appl. Phys. A*, **114**, 673–683.

Lopez-Arce, P., Gomez-Villalba, L.S., Pinho, L., Fernandez-Valle, M.E., Alvarez de Buergo, M., Fort, R. (2010): Influence of porosity and relative humidity on consolidation of dolostone with calcium hydroxide nanoparticles: effectiveness assessment with non-destructive techniques. *Mater. Character.*, **61**, 168–184.

Lopez-Arce, P., Gomez-Villalba, L.S., Martinez-Ramirez, S., Alvarez de Buergo, M., Fort, R. (2011): Influence of relative humidity on the carbonation of calcium hydroxide nanoparticles and the formation of calcium carbonate polymorphs. *Powder Technol.*, **205**, 263–269.

Martín Ramos, J.D. (2004): XPowder. A software package for powder X-ray diffraction analysis. Lgl. Dep. GR 1001/04.

Matteini, M. & Moles, A. (2003): La chimica nel restauro. I materiali dell'arte pittorica. Nardini Ed. 10th edition, Firenze, 147–168.

Natali, I., Tempesti, P., Carretti, E., Potenza, M., Sansoni, S., Baglioni, P., Dei, L. (2014): Aragonite crystals grown on bones by reaction of $CO_2$ with nanostructured $Ca(OH)_2$ in the presence of collagen. Implications in archaeology and paleontology. *Langmuir*, **30**, 660–668.

Rodrigues, J.D. & Grossi, A. (2007): Indicators and ratings for the compatibility assessment of conservation actions. *J. Cult. Herit.*, **8**, 32–43.

Rodriguez-Navarro, C., Suzuki, A., Ruiz-Agudo, E. (2013): Alcohol dispersions of calcium hydroxide nanoparticles for stone conservation. *Langmuir*, **29**, 11457–11470.

Ruffolo, S., La Russa, M.F., Aloise, P., Belfiore, C.M., Macchia, A., Pezzino, A., Crisci, G.M. (2014): Efficacy of nanolime in restoration procedures of salt weathered limestone rock. *Appl. Phys. A*, **114**, 753–758.

Salvadori, B. & Dei, L. (2001): Synthesis of $Ca(OH)_2$ nanoparticles from diols. *Langmuir*, **17**, 2371–2374.

UNE EN 1015–2 (1999): Methods of test for mortar for masonry—part 2: bulk sampling of mortars and preparation of test mortars. Spanish association for standardization and certification (AENOR), Madrid.

UNE EN 459–1 (2002): Description building lime—part 1: definitions, specifications and conformity criteria. Spanish association for standardization and certification (AENOR), Madrid.

UNE-EN 14579 (2005): ''Natural stone test methods. Determination of sound speed propagation.'' Spanish Association for Standardization and Certification (AENOR), Madrid.

The Venice Charter (1964): A bibliography. UNESCO-ICOMOS Documentation Centre – February 2012.

Ziegenbald, G. (2008): Colloidal calcium hydroxide – a new material for consolidation and conservation of carbonate stone. Proceedings of 11th International congress on deterioration and conservation of stone III, Lukaszewicz E & Niemcewicz P., eds., Torun, 1109–1115.

Zornoza-Indart, A., Lopez-Arce, P., Gomez-Villalba, L.S., Alvarez de Buergo, M., Varas-Muriel, M.J., Fort, R. (2012): Consolidation of deteriorated carbonate stones with nanoparticles of $Ca(OH)_2$. Proceedings of the 12th International Conference on the deterioration and conservation of stone. Columbia University, New York.

*Received 21 August 2014*
*Modified version received 23 December 2014*
*Accepted 7 January 2015*